The Scaling of the Diameter- and Thickness-Effect Curves for Ideal, Insensitive, and Non-Ideal Explosives

Scott I. Jackson and Mark Short

Shock and Detonation Physics Group, Los Alamos National Laboratory,
Los Alamos, NM 87544

1 Introduction and Summary

The geometry-dependent scaling of the detonation velocity with charge size has been a topic of recent interest [1–4] and has significant implications for condensed-phase explosive detonation propagation and failure dynamics. Initial efforts approximated classical detonation curvature theory to predict that the critical diameter and the diameter-effect curve of a cylindrical high-explosive (HE) charge should scale with twice the thickness t of an analogous two-dimensional HE slab [1–3]. The varied agreement of experimental results [1–4] with this prediction (hereafter referred to $d = 2t$) illustrated the need for a more rigorous analysis of the curvature terms on the detonation shock surface.

To address this inconsistency, we [5] previously used DSD-based (Detonation Shock Dynamics) D_n–κ theory to compare the detonation curvature associated with the cylindrical and slab rate stick geometries. Our analytical results showed that the $d = 2t$ scaling could only be expected to occur for very ideal explosives and that nonideal explosives would deviate significantly from the $d = 2t$ prediction. We also presented preliminary experimental results for the insensitive (slightly nonideal) explosive PBX 9502 that supported our conclusions by demonstrating that the detonation dynamics approached the $d = 2t$ scaling for large charge sizes (indicating ideal detonation), but deviated to a $d = 1.6t$ scaling near the failure diameter (where nonideal detonation occurs).

In the present study, we provide additional experimental data to further validate this theory. Numerous two-dimensional HE slab rate sticks have been fielded for explosives that exhibit ideal (PBX 9501), slightly nonideal (PBX 9502), and highly nonideal (ANFO) detonation. Detonation velocity versus slab thickness (thickness-effect curves) are compared to previous measurements for cylindrical rate sticks. Finally, the scale factor d/t necessary to overlay the diameter- and thickness-effect curves is computed for each explosive formulation. We observe that the scale factor varies with detonation velocity (or level of detonation "ideality"). Measured scale factors range from 1.89–2.20, 1.41–1.87, and 1.79–1.05 for PBX 9501, PBX 9502, and ANFO formulations, respectively, as detonation velocity D varies from the (near failure) critical velocity to the Chapman-Jouguet velocity D_{CJ}. These results further support our theoretical prediction [5] that the scale factor relating the diameter- and thickness-effect curves will increasingly deviate from two as the detonation structure becomes increasingly nonideal.

2 Size Effect and Wavefront Curvature Theory

It has long been known that the detonation phase velocity D of a condensed-phase explosive will decrease with increasing flow divergence in the detonation reaction zone (RZ) [6]. This divergence occurs when post-shock pressures exceed the yield stress of the HE's confiner and results in the transverse expansion of flow behind the shock front (Fig. 1). The onset of transverse flow ahead of the sonic locus induces curvature of the shock front. As the charge diameter d decreases, so does the ratio of the energy driving the shock relative to the energy lost

to flow expansion, resulting in a decreased D. In cylindrical charges, this velocity decrement with diameter is referred to as an HE's diameter effect. We refer to the analogous curve for the slab geometry as the "thickness effect" and both curves together as the "size effect." Figure 2 shows an example of this behavior from Ref. [7] for neat nitromethane (NM) and a NM-silica-guar mixture. The decreased detonation velocities and flow divergence can decrease the post-shock temperatures and delay more of the chemical energy release to behind the sonic locus of the RZ. The detonation will fail below a critical limit where detonation shock and RZ coupling can no longer be maintained. In practice, the charge diameter corresponding to this limit is defined as the failure diameter d_c. Such losses can also be present in gas-phase detonation [8], although in controlled experiments the lower pressures achieved in gas-phase detonation rarely exceed the yield stress of most metal confiners. However, flow divergence can still result from frictional and thermal losses in the RZ flow [9] and have a measurable effect on D as the tube diameter approaches the RZ length.
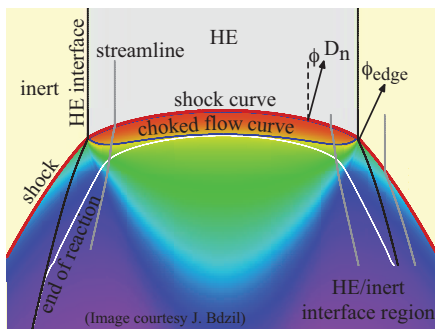

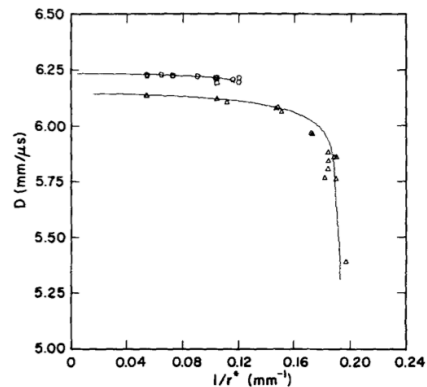Fig. 1: Flow divergence and curvature.

Fig. 2: Diameter effect for NM mixtures [7].

3   Experimental Data and Results

The slab-geometry experiments were designed to generate a region of two-dimensional quasi-steady flow, over which detonation velocities and front shapes could be measured. The experimental geometry was an unconfined variant of the detonation sandwich test [10, 11]. Shown in Fig. 3, the experiment consisted of a high-aspect-ratio rectangular-cuboid main charge that was boosted by a detonation line wave generator [12, 13].
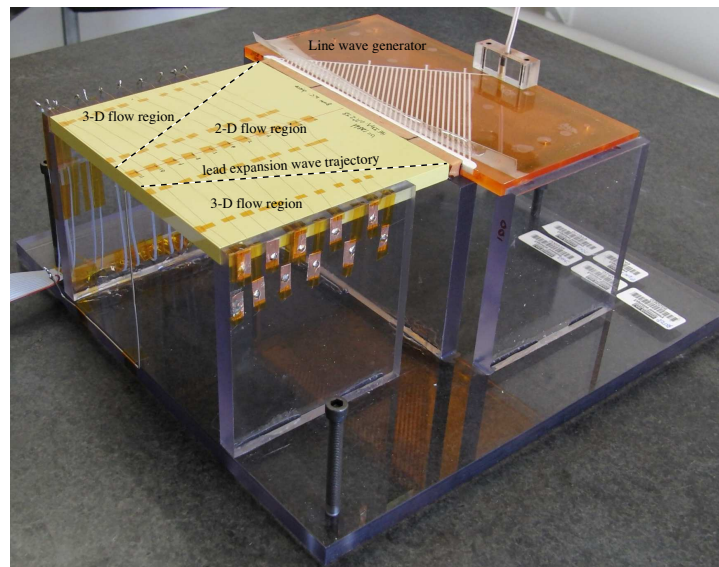

Fig. 3: The slab rate stick geometry for a PBX 9502 test.

The line wave generator consists of a series of intersecting channels designed such that the distance from the initiation point to the output line is identical for all detonation paths through the device. During operation, a point detonator initiates a detonation in the main channel of the line wave generator, which spreads throughout the device and generates a linear detonation wave at the output line. That linear detonation wave then propagates through a rectangular-cuboid booster pad that is composed of an explosive with sufficient output strength to promptly initiate a linear detonation wave into the adjacent main charge. The detonation then propagates along the main charge to a front shape measurement surface located at the centerline (across the thinnest dimension) of the output face. Time-of-arrival pins or wires track the phase velocity D of the detonation along the main charge side wall.

For a perfectly linear detonation input, the main charge contains a region of two-dimensional flow in the shape of an isosceles trapezium (as indicated by dashed lines in Fig. 3). The transverse expansion of the higher-pressure detonation products into the confiner propagates an expansion fan towards the main charge centerline at the detonation RZ sound speed. Detonation regions in the interior portion of the main charge do not experience any transverse expansion in the width dimension and are considered two-dimensional in nature. Regions of the wave that are behind the lead transverse expansion wave will exhibit three-dimensional flow. Thus, main charge dimensions must be selected such that a two-dimensional region is maintained over the time-of-arrival pin and front-shape measurement region. Jackson and Short [14] performed experiments and analysis that verified the presence of a large two-dimensional flow region at the downstream shock breakout surface for charges with similar aspect ratios to the present experiments.

Additionally, the axial charge length in the direction of detonation propagation must be sufficiently long that a steady two-dimensional detonation velocity can be achieved. Typically, this requires a length of several charge thicknesses to damp out any booster overdrive or underdrive and for the two-dimensional flow to be established. The present experiments were generally at least 10 charge thicknesses in length to allow for a steady-state two-dimensional detonation velocity. Thus, charges should be as long as possible to achieve a steady-state velocity and as wide as possible to maintain a sufficient two-dimensional measurement region. For less sensitive explosives with larger reaction zones (such as ANFO), these two considerations require very large charges compared to more sensitive formulations.

Nine, seven and three slab experiments were performed with the PBX 9501, PBX 9502 and ANFO formulations, respectively. Ionization or shorting probes were used as the time-of-arrival diagnostics. For each test, either 11 or 22 ionization probes were located on the main charge. Probe position x_i and detonation arrival time t_i data were fit to a line ($x = Dt + t_0$) using a least-squares fit optimization. The slope of the line was the steady-state detonation velocity. For all tests, the detonation velocity was seen to increase with slab thickness. Standard error values were generally $0.2\% D$, indicating steady detonation.

Figure 4 shows the slab diameter-effect (red) points compared to previously obtained data from cylindrical rate sticks (blue) for PBX 9501. Several curves are also plotted. The red and blue curves are fits to the slab and cylinder experimental data, respectively, using the empirical short Erying form

$$D = D_{CJ}\left(1 - \frac{A}{R - R_c}\right) \tag{1}$$

and substituting the independent variable R with cylinder diameter d or slab thickness t depending on the test geometry. Parameters A and R_c were fitting parameters. The green (dashed) curve is the slab curve fit reparameterized with the $d = 2t$ scaling. For the PBX 9501 data, this $1/2t$ (green) curve agrees well with the $1/d$ (blue) curve and indicates good agreement with the $d = 2t$ scaling.

Equivalent plots are shown for PBX 9502 and ANFO in Figs. 5 and 6. For all plots, the measured detonation velocities in the slabs are seen to be higher than that of the cylinders for equivalent charge sizes (i.e. where $d = 2t$). However, with these less ideal explosives, more significant deviations are seen from the $d = 2t$ scaling. The PBX 9502 data (Fig. 5) indicates near $d = 2t$ scaling for large charges (low values of $1/d$ and $1/t$) but varies significantly from the $d = 2t$ scaling as the charge size decreases (increasing values of $1/d$ and $1/t$). This is consistent with the operation of an insensitive explosive, which exhibits increasingly nonideal detonation with decreasing charges sizes. The highly nonideal ANFO data (Fig. 6) does not exhibit the $d = 2t$ anywhere on the size-effect plot.

The scaling factor can be computed by solving the Eyring equation fits for $d(D)$, $t(D)$, and then computing d/t versus D. The computed scaling for all three explosive formulations is shown in Fig. 7 as a function of
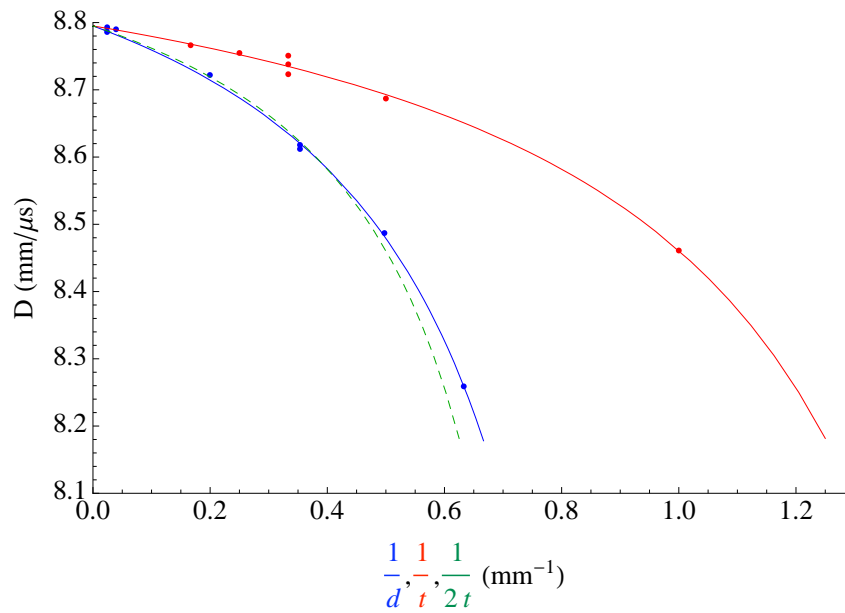
Fig. 4: The diameter-effect ($1/d$, blue) and thickness-effect ($1/t$, red) curves for PBX 9501. The $1/2t$ (dashed, green) curve illustrates the idealized $d = 2t$ scaling.
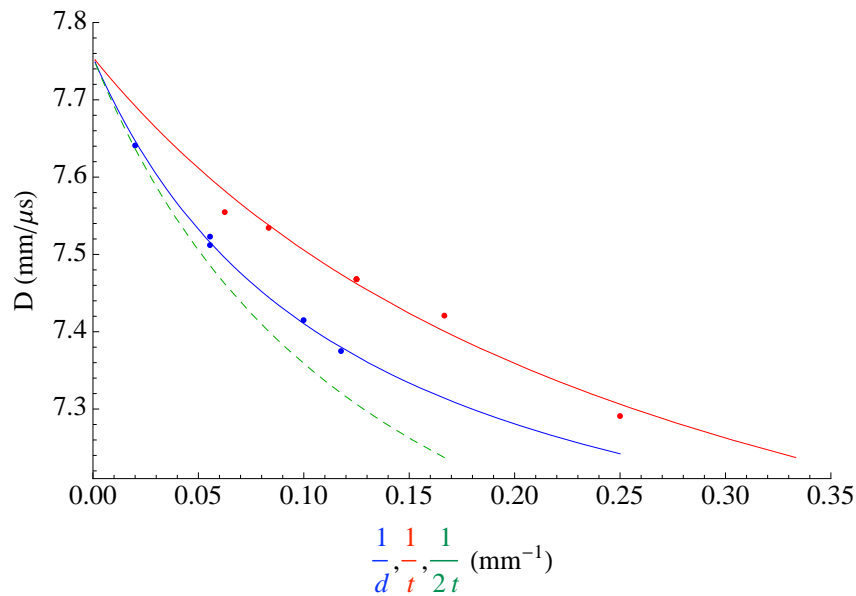

Fig. 5: The diameter-effect ($1/d$, blue) and thickness-effect ($1/t$, red) curves for PBX 9502. The $1/2t$ (dashed, green) curve illustrates the idealized $d = 2t$ scaling.
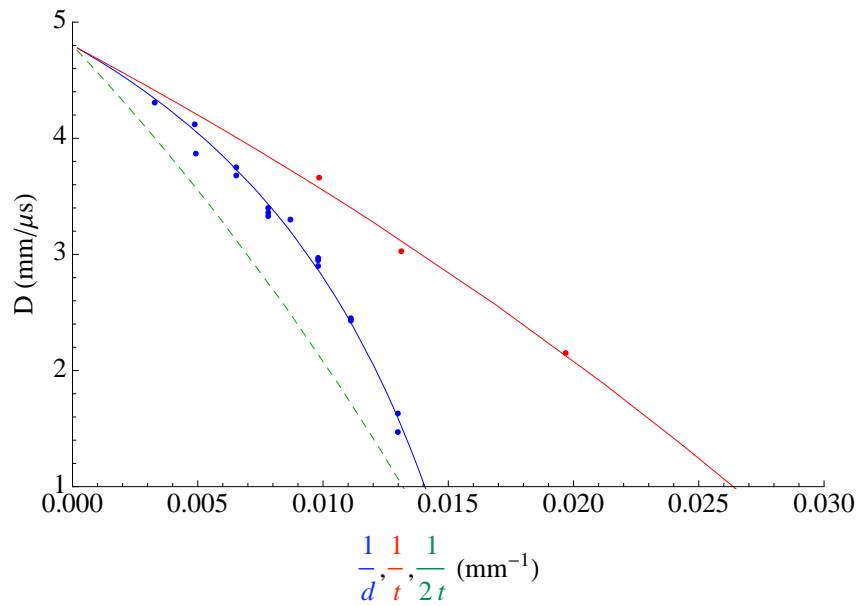
Fig. 6: The diameter-effect ($1/d$, blue) and thickness-effect ($1/t$, red) curves for ANFO. The $1/2t$ (dashed, green) curve illustrates the idealized $d = 2t$ scaling.
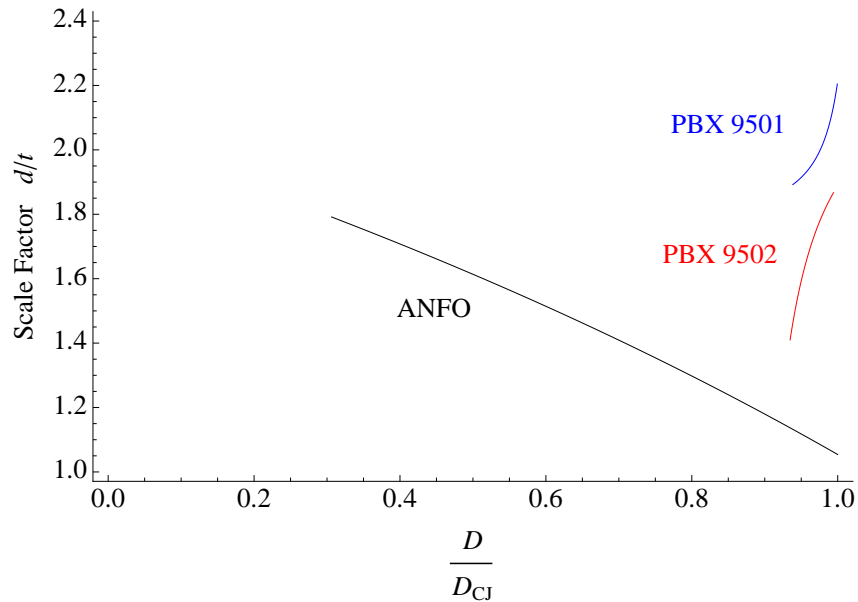

Fig. 7: Computed scale factors from the experimental data for PBX 9501 (blue), PBX 9502 (red) and ANFO (black).

normalized detonation velocity D/D_{CJ}. As was indicated on the size-effect plot, the PBX 9501 (blue line) scale factor ranges from 1.89–2.20 as the detonation velocity increases from near failure (8.26 mm/μs) to the CJ velocity (8.79 mm/μs). As expected for an ideal explosive, this scale factor range is consistent with the $d = 2t$ scaling.

The PBX 9502 scale factor (red line) ranges from 1.41–1.87 as the detonation velocity increases from the critical value (7.29 mm/μs) to the CJ velocity (7.76 mm/μs). As discussed, these data indicate that the PBX 9502 detonation only approaches the $d = 2t$ scaling at large charge sizes. The ANFO scale factor (black line) ranges from 1.79–1.05 as the detonation velocity increases from the lowest measured value (1.49 mm/μs) to the CJ velocity (4.80 mm/μs). This result deviates significantly from the $d = 2t$ scaling.

In our presentation, we will discuss the experimental data and Eyring fits in more detail, compare our measured scale factors with those found in previous studies, and discuss the implications of these results for DSD prediction and detonation failure dynamics.

References

[1] O. Petel, D. Mack, A. Higgins, R. Turcotte, and S. Chan, "Minimum propagation diameter and thickness of high explosives," Journal of Loss Prevention in the Process Industries, vol. 20, pp. 578–583, 2007.

[2] V. V. Silvestrov, A. V. Plastinin, S. M. Karakhanov, and V. V. Zykov, "Critical diameter and critical thickness of an emulsion explosive," Combustion, Explosion, and Shock Waves, vol. 44, no. 3, pp. 354–359, 2008.

[3] A. Higgins, "Measurement of detonation velocity for a nonideal heterogenous explosive in axisymmetric and two-dimensional geometries," in Shock Compression of Condensed Matter, pp. 193–196, American Institute of Physics, 2009.

[4] J. Gois, J. Campos, and R. Mendes, "Extinction and initiation of detonation of NM-PMMA-GMB mixtures," in Shock Compression of Condensed Matter, pp. 827–830, American Institute of Physics, 1996.

[5] S. Jackson and M. Short, "Geometry-specific scaling of detonation parameters from front curvature," in Proceedings of the 23rd International Colloquium on the Dynamics of Explosions and Reactive Systems, (Irvine, CA), July 24–29 2011.

[6] H. Jones, "A theory of the dependence of the rate of detonation of solid explosives on the diameter of the charge," Provc. Royal Soc., Series A, vol. 1018, pp. 415–426, 1947.

[7] R. Engelke and J. Bdzil, "A study of the steady-state reaction-zone structure of a homogenous and a heterogenous explosive," Physics of Fluids, vol. 26, pp. 1210–1221, 1983.

[8] E. Dabora, J. Nicholls, and R. Morrison, "Influence of a compressible boundary on propagation of gaseous detonations," in Proceedings of the 10th International Symposium on Combustion, vol. 10, (Pittsburgh, PA), pp. 817–830, Combustion Institute, 1965.

[9] J. Fay, "Two-dimensional gaseous detonations: Velocity deficit," Physics of Fluids, vol. 2, pp. 283–289, 1959.

[10] L. G. Hill and T. D. Aslam, "The lanl detonation-confinement test: Prototype development and sample results," AIP Conference Proceedings, vol. 706, no. 1, pp. 847–850, 2004.

[11] T. D. Aslam, J. B. Bdzil, and L. G. Hill, "Analysis of the lanl detonation-confinement test," AIP Conference Proceedings, vol. 706, no. 1, pp. 831–834, 2004.

[12] S. Jackson, J. Austin, and J. Shepherd, "Planar detonation wave initiation in large-aspect-ratio channels," AIAA Journal, vol. 44, no. 10, pp. 2422–2425, 2006.

[13] J. Morris, S. Jackson, and L. Hill, "A simple line wave generator using commercial explosives," in Shock Compression of Condensed Matter - 2009, vol. 1195 of AIP Conference Proceedings, (Melville, NY), pp. 408–411, American Institute of Physics, 2009.

[14] S. Jackson and M. Short, "Determination of the velocity-curvature relationship for unknown front shapes," in Shock Compression of Condensed Matter - 2011, vol. 1426 of AIP Conference Proceedings, (Melville, NY), pp. 347–350, American Institute of Physics, 2012.